**Atmospheric
Chemistry
and Physics**

# Tropospheric ozone variations at the Nepal Climate Observatory-Pyramid (Himalayas, 5079 m a.s.l.) and influence of deep stratospheric intrusion events

P. Cristofanelli[1], A. Bracci[1,2], M. Sprenger[2], A. Marinoni[1], U. Bonafè[1], F. Calzolari[1], R.Duchi[1], P. Laj[3], J.M. Pichon[4], F.Roccato[1], H. Venzac[4], E.Vuillermoz[5], and P. Bonasoni[1,5]

[1]Institute for Atmospheric Science and Climate, National Research Council, Bologna, Italy
[2]ETHZ, Zurich, Switzerland
[3]Laboratoire de Glaciologie et Géophysique de l'Environnement, St Martin d'Hères Cedex, France
[4]Laboratoire de Meteorologie Physique, CNRS, Université Blaise Pascal, Aubiere cedex, France
[5]EV-K2-CNR Committee, 24126 Bergamo, Italy

**Abstract.** The paper presents the first 2 years of continuous surface ozone ($O_3$) observations and systematic assessment of the influence of stratospheric intrusions (SI) at the Nepal Climate Observatory at Pyramid (NCO-P; $27°57'$ N, $86°48'$ E), located in the southern Himalayas at 5079 m a.s.l.. Continuous $O_3$ monitoring has been carried out at this GAW-WMO station in the framework of the Ev-K2-CNR SHARE and UNEP ABC projects since March 2006. Over the period March 2006–February 2008, an average $O_3$ value of $49\pm12$ ppbv ($\pm1\delta$) was recorded, with a large annual cycle characterized by a maximum during the pre-monsoon ($61\pm9$ ppbv) and a minimum during the monsoon ($39\pm10$ ppbv). In general, the average $O_3$ diurnal cycles had different shapes in the different seasons, suggesting an important interaction between the synoptic-scale circulation and the local mountain wind regime.

Short-term $O_3$ behaviour in the middle/lower troposphere (e.g. at the altitude level of NCO-P) can be significantly affected by deep SI which, representing one of the most important natural input for tropospheric $O_3$, can also influence the regional atmosphere radiative forcing. To identify days possibly influenced by SI at the NCO-P, a specially designed statistical methodology was applied to the time series of observed and modelled stratospheric tracers. On this basis, during the 2-year investigation, 14.1% of analysed days were found to be affected by SI. The SI frequency showed a clear seasonal cycle, with minimum during the summer monsoon

(1.2%) and higher values during the rest of the year (21.5%). As suggested by back-trajectory analysis, the position of the subtropical jet stream could play an important role in determining the occurrence of deep SI transport on the southern Himalayas.

We estimated the fraction of $O_3$ due to SI at the NCO-P. This analysis led to the conclusion that during SI $O_3$ significantly increased by 27.1% (+13 ppbv) with respect to periods not affected by such events. Moreover, the integral contribution of SI ($O_{3S}$) to $O_3$ at the NCO-P was also calculated, showing that up to 13.7% of $O_3$ recorded at the measurement site could be possibly attributed to SI. On a seasonal basis, the lowest SI contributions were found during the summer monsoon (less than 0.1%), while the highest were found during the winter period (up to 24.2%). Even considering the rather large uncertainty associated with these estimates, the obtained results indicated that, during non-monsoon periods, high $O_3$ levels could affect NCO-P during SI, thus influencing the variability of tropospheric $O_3$ over the southern Himalayas.

## 1 Introduction

Even if about 90% of atmospheric $O_3$ molecules resides in the stratosphere, tropospheric $O_3$ strongly influences the radiative budget of the atmosphere (Forster et al., 2007) and the oxidation capacity of the troposphere (Gauss et al., 2003). Due to its high chemical reactivity in the lower troposphere, $O_3$ is considered a dangerous pollutant, causing harm to human health (e.g. Hoek et al., 1993; Conti et al., 2005) and

ecosystems (e.g., Fuhrer and Booker, 2003; Paoletti et al., 2006), while in the free troposphere it has been recognised as the third greenhouse gas in terms of anthropogenic radiative forcing (Forster et al., 2007). Although the greatest contribution to tropospheric $O_3$ today comes from photochemical production (e.g. Jacobson, 2002), other concurring processes like Stratosphere-Troposphere Exchange (STE) cannot be neglected (e.g. Roelofs and Lelieveld, 1997; Wild, 2007; Trickl et al., 2010). As a result of the interaction of these processes with air-mass transport (both regional and long range), and due to its variable chemical lifetime (from days to a month), tropospheric $O_3$ exhibits complex spatial and temporal variations that lead to an inhomogeneous distribution of its radiative forcing (Mickley et al., 2004) and non-linear effects on regional air quality (West et al., 2009). Thus, it is crucial to evaluate in detail the processes able to influence $O_3$ behaviour. Due to the increasing emissions of anthropogenic $O_3$ precursors (Ohara et al., 2007), the issue appears especially urgent with regard to South Asia, where a vast region extending from the Indian Ocean to the Himalayas is characterised by the presence of copious amounts of aerosol and pollutant gases (the so-called Atmospheric Brown Cloud), with severe implications on regional climate, air-quality and food safety (Ramanathan et al., 2008). In particular, there is still a gap in knowledge concerning the typical levels and variations of tropospheric $O_3$ over the high Himalayas where, besides influencing the mountain ecosystem air quality, it can strongly contribute to the atmospheric heating of absorbing aerosols in the Brown Cloud (Ramanathan et al., 2008).

For these reasons and with purpose of contributing to filling this gap in knowledge, this work presents the first complete description of surface $O_3$ behaviours at the WMO-GAW station "Nepal Climate Observatory – Pyramid" (NCO-P, 5079 m a.s.l., Nepal), together with a systematic evaluation of the role of deep stratospheric intrusions in determining the observed $O_3$ levels. At this station, in the framework of the UNEP ABC (Atmospheric Brown Clouds) and Ev-K2-CNR SHARE (Stations at High Altitude for Research on the Environment) projects, since March 2006 high quality continuous measurements of trace gases, aerosol and meteorological parameters have been conducted, in order to attain a detailed characterization of the background tropospheric composition and variability over the remote South Himalayas. Thus, together with the work by Bonasoni et al. (2010) that will focus on polluted air-mass transport, the present paper better clarifies the role played by transport processes in determining the $O_3$ levels and variability in one of the most critical high-altitude regions. It should well clarify that part of this work is aimed in evaluating the contribution of relatively "fresh" stratospheric inputs, i.e. still having a clear fingerprint of their stratospheric origin. Nevertheless, this experimental investigation can also provide useful hints for better evaluating the capacity of global and regional models in assessing the current tropospheric $O_3$ levels, and

its climatic effect in this important world area. In fact, high mountain stations are appropriate locations for investigating the episodic transport of stratospheric air-masses deep into the troposphere (e.g. Elbern et al., 1997; Stohl et al., 2000), as well as representing very suitable sites for the study tropospheric background conditions (e.g. Wotawa et al., 2000; Henne et al., 2008). Signal of stratospheric air-masses have been detected by Wang et al. (2006) by analysing $O_3$ and CO values recorded during a summer campaign in the northeastern Qinghai-Tibetan Plateau (Mt. Waliguan, 26.3° N, 100.9° E, 3816 m a.s.l.). At the same measurement site, by analysing case studies, Ding and Wang (2006) suggested that stratospheric intrusions can play an important role during summer but without providing any estimate of the possible contribution to $O_3$ levels. Concerning the Mt. Everest region, by analysing single case studies and long-term satellite measurements, Moore and Semple (2004) indicated that SI can trigger extreme weather events at the mountain peak, also speculating that the interaction of the Tibetan Plateau with large-scale circulation can favour STE over South Himalayas (Moore and Semple, 2005). By analysing data from two field campaigns, Zhu et al. (2006) suggested that high $O_3$ in the northern slope of Mt. Everest could be attributed to katabatic winds pumping down $O_3$ rich air-masses from upper air levels. More recently, by analysing the first round-year of continuous $O_3$ measurement at NCO-P, Cristofanelli et al. (2009) evaluated that during 25 SI days the daily $O_3$ mixing ratio increased by 9.3% compared to seasonal values.

To detect experimentally stratospheric intrusion (SI) events at a specific surface measurement site or throughout the troposphere, the temporal variations of specific stratospheric tracers can be analysed. SI is often related to frontal activity, leading to the development of tropopause folds (e.g. Sprenger et al., 2003), deep troughs (e.g. Davies and Schuepbach, 1994) and cut-off lows (e.g. Sprenger et al., 2007) at upper levels, as well as rapid cyclones (e.g. Loring et al., 1996), fronts or high-pressure systems at the surface (e.g. Davies and Schuepbach, 1994). For this reason, concomitant atmospheric pressure (AP) variations are often observed at measurement sites when SI occurs. Several authors (e.g. Sprenger et al., 2007) have used Ertl's potential vorticity (PV) to diagnose the presence of stratospheric air deep into the troposphere. In fact, in the atmosphere above 350 hPa, PV rapidly increases with altitude, reaching typical values above 1.0 pvu (Danielsen, 1968) at the tropopause level (where $1 \text{ pvu} = 10^{-6} \text{ m}^2 \text{ K kg}^{-1} \text{ s}^{-1}$), thus representing a valid stratospheric tracer under adiabatic and frictionless flows. The detection of high values of total column ozone (TCO) over a specific location or the identification of strong TCO horizontal gradients can also be used to identify SI (e.g. Olsen et al., 2000; Wimmers et al., 2004).

Along with high $O_3$ concentrations and PV values, stratospheric air is also characterised by low water vapour contents and low anthropogenic pollutants (e.g. black carbon). For this reason the experimental recognition of SI at high
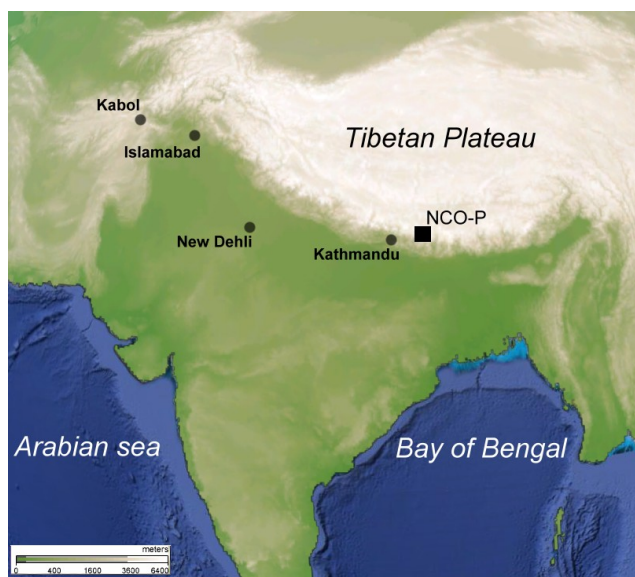
**Fig. 1.** NCO-P geographical location. Adapted from www. earthobservatory.nasa.gov.

mountain sites is often additionally based on the identification of "clean" and low RH conditions (e.g. Stohl et al., 2000; Trickl et al., 2010).

The work presents and analyses surface $O_3$ measurements continuously recorded at NCO-P from 1 March 2006 to 18 February 2008. In particular, by applying a specially designed selection methodology based on the analysis of insitu data ($O_3$, AP, RH), satellite TCO data and 3-D air-mass back-trajectories, the days possibly influenced by SI were accurately identified. Here we extend the previous work by Cristofanelli et al. (2009) with the principal aim of characterizing the surface $O_3$ behaviours in South Himalayas and further investigating SI seasonal cycle and estimating the SI contribution to the observed $O_3$ levels .

## 2 Methods

### 2.1 Measurement site and in-situ observations

The NCO-P (27°57′ N, 86°48′ E) is located at 5079 m a.s.l., in the southern Himalayas (Fig. 1) at the confluence of two glacial valleys: Lobuche and Khumbu. As shown by Bonasoni et al. (2010), the air-mass circulation at this measurement site is strongly influenced both by the synoptic scale circulation and the local mountain wind regime. The interaction between these components leads to the onset and decay of the summer monsoon and winter season reported by Bonasoni et al. (2010) and adopted also in this work to define seasonal transitions during the years (Table 1). In particular, up-valley breezes can favour the transport of polluted air-masses rich in $O_3$ and BC from lower altitude regions.

For this reason, particular attention was devoted to ensuring that the $O_3$ levels observed during the identified SI days were not influenced by anthropogenic emissions. In particular, as shown in Section 5 below, surface $O_3$ data were analysed as a function of RH and black carbon (BC), to prevent moist and polluted air-masses influencing the analysed measurements. Surface $O_3$ measurements (Fig. 2) have been continuously performed with a UV-photometric analyser (Thermo Scientific – Tei 49C), adopting the sampling procedures suggested within the GAW-WMO (GAW, 1992). During a maintenance campaign in February 2007, the instrument was compared against a travelling standard by GAW/WCC at EMPA (World Calibration Centre for Surface Ozone, Carbon Monoxide and Methane at the Swiss Federal Laboratories for Materials Testing and Research). In agreement with Klausen et al. (2003), the combined standard uncertainty (1-min basis) was ascertained to be less than ±1.5 ppbv in the range 0–100 ppbv. At NCO-P, equivalent BC concentrations are determined using a multi-angle absorption photometer (MAAP 5012, Thermo Electron Corporation). This instrument measures the absorption coefficient of aerosol deposited on a glass fibre filter tape, also removing the scattering effect at different angles, which can interfere with optical absorption measurements. The reduction of light transmission at 670 nm, multiple reflection intensities, and air sample volume are continuously integrated over the sample run period to provide a real time output (1-min resolution) of equivalent BC concentration (Petzold et al., 2002). For further details on BC measurements and typical behaviours at NCO-P, please refer to Marinoni et al. (2010). At NCO-P, conventional meteorological parameters are continuously recorded by means of an integrated weather station (Vaisala WXT-410). In particular, AP shows a small variability during the year (standard deviation: 3.6 hPa) with an average value of 550.9 hPa. As shown in Fig. 2, the yearly AP cycle was characterised by higher (and less variable) values from June to October (552.2±0.6 hPa) and lower (and more variable) values from November to March (547.7±3.1 hPa). This behaviour appeared to be strongly affected by the so-called "Tibetan High", a strong thermal anticyclone forming in the upper troposphere during the monsoon season, while for the rest of the year the passage of eastward propagating synoptic disturbances mainly determine AP variations at the measurement site (Böhner, 2006). All the in-situ parameters presented in this paper are reported at local time (LT, i.e. UTC+5.45), unless otherwise reported, while all concentrations refer to STP conditions (273 K and 1013 hPa).

### 2.2 Back-trajectory calculation

In order to determine the origin of air masses reaching NCO-P, 5-day back-trajectories starting at the measurement site were calculated every 6 h (at 00:00, 06:00, 12:00 and 18:00 UTC) with the Lagrangian Analysis Tool LA-GRANTO (Wernli and Davies, 1997). To minimize possible
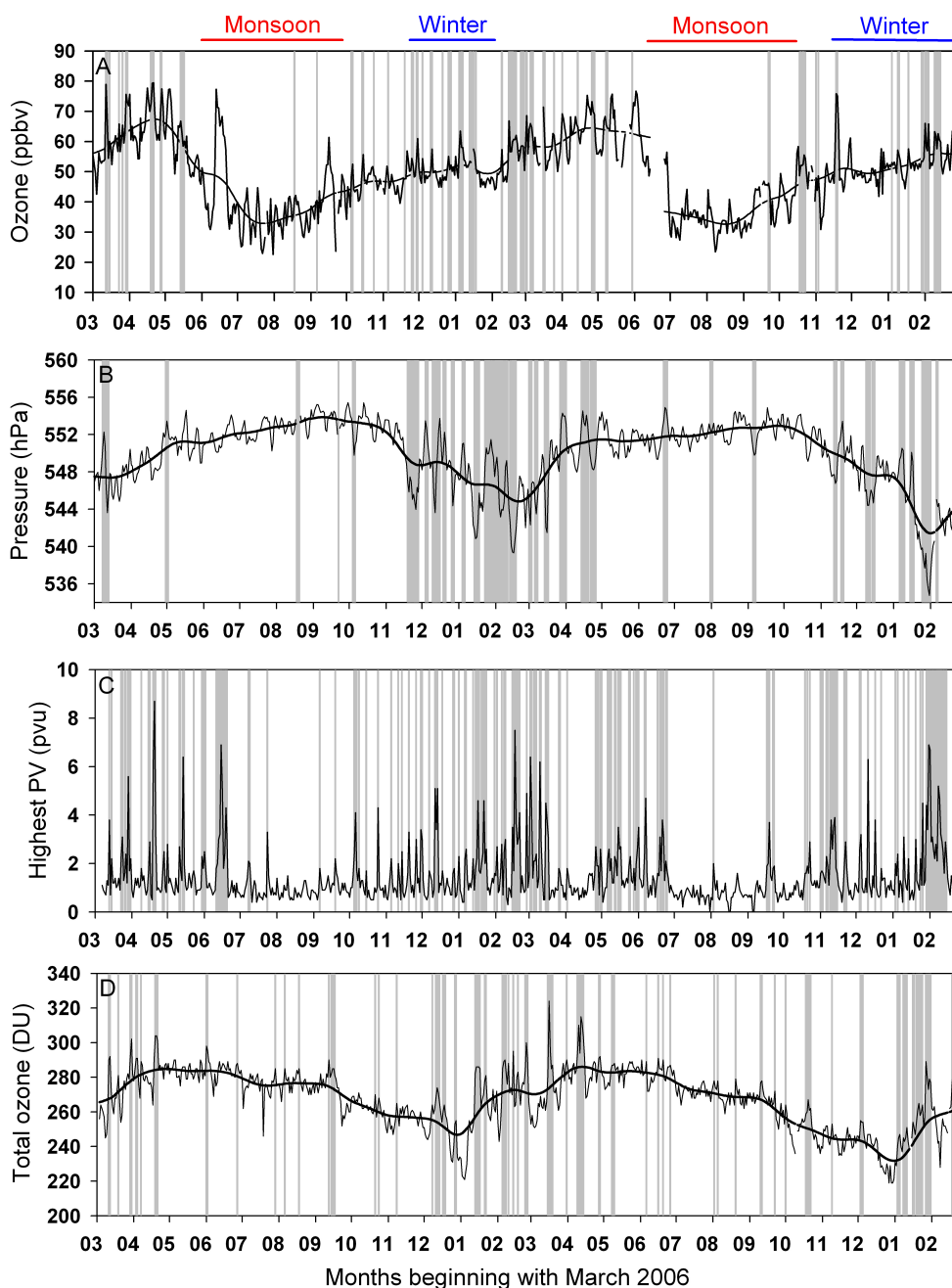
**Fig. 2.** Time series (daily average values) of surface $O_3$ **(A)**, atmospheric pressure **(B)**, maximum potential vorticity over 14 back-trajectories extending up to 50 hPa over the measurement site altitude **(C)** and total column ozone **(D)** from March 2006 to February 2008. For surface $O_3$, atmospheric pressure and total $O_3$, the thick lines represent the seasonal behaviour obtained by applying the KZ filtering. The vertical grey bars denote the days characterised by parameter values exceeding the threshold for detection of SI events. Top horizontal coloured bars denote winter and monsoon seasons.

effects of the differences between model and real topography, the 3-D trajectories were started at the pressure level of 530 hPa, which almost corresponds to the station height above sea level. Trajectory calculations were based on the 6-hourly meteorological 3D grid field composing the operational analysis produced by the European Centre for Medium

Range Weather Forecasts (ECMWF). The 3-D wind fields were interpolated onto a horizontal $1° \times 1°$ grid. Subgrid scale processes, like convection and turbulent diffusion, are not represented by LAGRANTO back-trajectories. To compensate partially for such uncertainties, and also to evaluate the coherence of flow, which depends strongly on the

**Table 1.** Identification of season transitions as a function of the local weather regime at NCO-P (from Bonasoni et al., 2010)

| Year | Season | Start day–End day |
|------|--------|-------------------|
| 2006 | Pre-monsoon | 1 March–20 May |
|      | Monsoon | 21 May–26 September |
|      | Post-monsoon | 27 September–20 November |
|      | Winter | 21 November 2006–31 January 2007 |
| 2007 | Pre-monsoon | 1 February–5 June |
|      | Monsoon | 6 June–12 October |
|      | Post-monsoon | 13 October–14 November |
| 2008 | Winter | 15 November–18 February 2008 |



**Fig. 3.** Box-and-whiskers analysis of daily $O_3$ means for months from March 2006 to February 2008. The box and whiskers denote the 10th, 25th, 50th, 75th and 90th percentiles, the outliers the 5th and 95th percentiles and the bold lines the average values.

3-D flow structure and temporal evolution, in addition to the backward trajectory started at the NCO-P location, 6 additional back-trajectories with endpoints shifted by $\pm1°$ in latitude/longitude and $\pm50$ hPa in pressure were also considered.
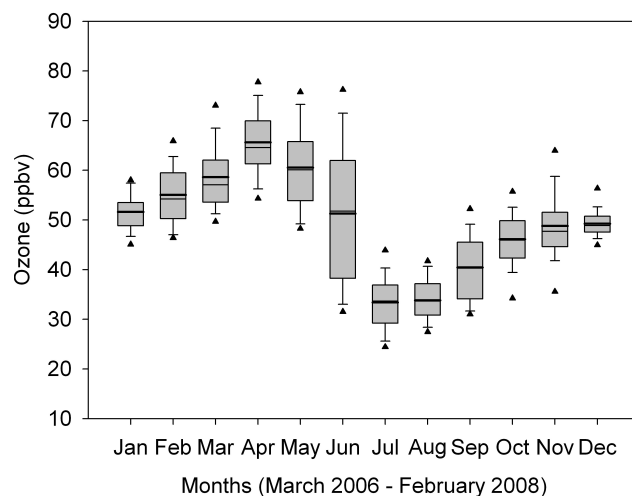
For every point along the trajectory (interpolated at a time resolution of 2 h), the model provides the geographic location and altitude of the air parcel, as well as other important physical quantities, like Ertel's PV, which can facilitate the identification of stratospheric air-masses. For each analysed day, the highest PV values along the 14 back-trajectories ending up to 50hPa above the receptor point are shown in Fig. 2. It is evident that the highest PV values related to air-masses reaching the measurement site from October to mid-June, with lower values during the monsoon season.

## 2.3 Ozone Monitoring Instrument (OMI) data

Daily total column $O_3$ (TCO) from the Dutch-Finnish Ozone Monitoring Instrument (OMI) (Levelt et al., 2006a, b) on board the NASA Earth Observing System Aura satellite (Schoeberl et al., 2006) were analysed for the NCO-P location (pixel extension: $1.00°$ Lat. $\times 1.25°$ Long.; local time overpass: $\sim12:00$ LT). In particular, TCO showed a clear seasonal behaviour (Fig. 2) characterized by low values from late September to early January ($255\pm11$ DU) and high values during the pre-monsoon period ($278\pm13$ DU). These variations are related to different controlling factors (Han et al., 2001; Tian et al., 2008): i.e. variations of large scale circulation, eddy transport, and chemical sources/sinks (Miyazaki et al., 2005).

## 3 Surface $O_3$ behaviour at NCO-P

The $O_3$ measurements at NCO-P represent the longest continuous $O_3$ time series recorded at an high-altitude Himalayan location. For the considered period, the surface $O_3$ mean concentrations gave a value of $49\pm12$ ppbv; N: 696 ($\pm1\sigma$; N being the number of data). As shown by the analysis of daily mean values (Fig. 3), the seasonal cycle of $O_3$

showed maxima during pre-monsoon periods (average mean value: $61\pm9$ ppbv; N: 202) and minima during the monsoon seasons ($39\pm10$ ppbv; N: 247). The spring (pre-monsoon) maximum with a summer (monsoon) minimum is typical for seasonal $O_3$ cycles at other locations in South/South-East Asia (e.g. Wahid et al., 2001; Tanimoto et al., 2005; Agrawal et al., 2008), where the monsoon regime strongly influences atmospheric circulation. As shown by Bonasoni et al. (2010), while the seasonal $O_3$ minima during the monsoon period are related to the northward transport of air masses poor in $O_3$ from the Indian subcontinent and ocean, other processes can contribute to explaining the higher $O_3$ levels recorded during the remaining seasons. In particular, during the pre-monsoon period, both SI and long-range/regional transport from Central Asia, North Africa and Middle East (Wang et al., 2006; Sudo and Akimoto, 2007; Bonasoni et al., 2010) can contribute to the observed $O_3$ concentrations. In addition to long-range transport, a not-negligible source of $O_3$ may also be the local/regional transport of air-masses rich in anthropogenic pollutants and biomass burning products (Bonasoni et al., 2008). In fact, the efficient valley wind circulation characterising the Khumbu region represents a favoured channel for the injection of pollution to the high Himalayas (Bonasoni et al., 2010). The influence of the mountain wind regimes on $O_3$ concentrations was investigated by considering the average diurnal variation of normalized $O_3$ values obtained by subtracting daily means from the actual 30-min $O_3$ concentrations (Fig. 4). With the purpose of stressing the day-to-day variability that can affect the diurnal cycle of $O_3$ at this measurement site, also the 25th and 75th percentiles of the normalized $O_3$ values ($\Delta O_3$) have been calculated. As shown by this elaboration, it should be noted
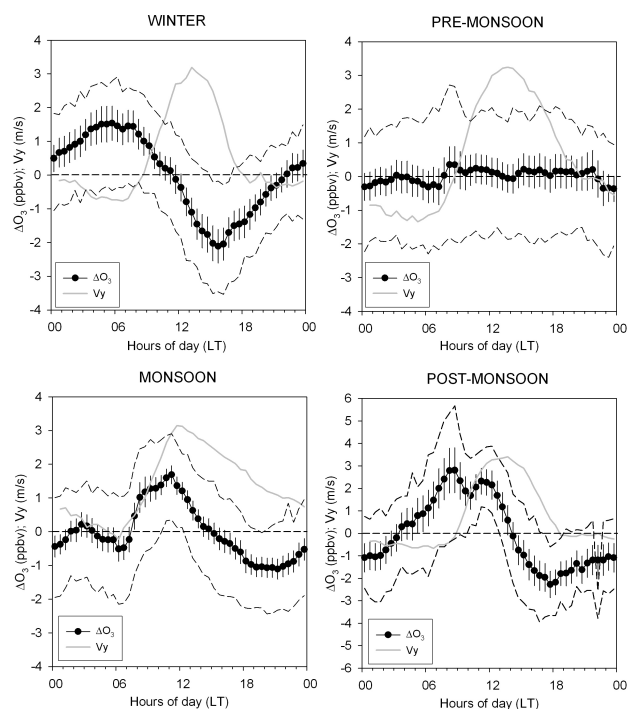
**Fig. 4.** Diurnal cycle of normalized $O_3$ values ($\Delta O_3$) and meridional wind component ($V_y$) for the different seasons at the NCO-P. The vertical bars denote the 95% confidence level while the upper and lower dotted lines denote the 25th and 75th percentiles for $\Delta O_3$.

that the actual amplitude of single day cycles can be significantly higher than the "smoothed" amplitudes of the averaged diurnal cycles. In general, the average $O_3$ diurnal cycles presented different shapes for the different seasons. During the winter season, a day-time minimum (16:00–17:00) and a night-time maximum (04:00–05:00) were observed. The average behaviour of the in-situ meridional wind component ($V_y$), clearly indicated that up-valley winds ($V_y > 0$ m/s) usually dominated during day-time and down-valley winds ($V_y < 0$ m/s) during night-time. This suggests that the day-time $O_3$ minimum can be attributed to the advection of air-masses from the ABL, which, due to surface dry deposition or possible enhanced titration, could be characterised by lower $O_3$ concentrations with respect to air-masses more representative of the free troposphere. On the other hand, the day-time $O_3$ minimum might also be due to $O_3$ loss by surface deposition along the valley floor or in-situ photochemical destruction under low nitrogen oxide ($NO_x$) conditions, which are likely at high-mountain sites (e.g. Fischer et al., 2003; Henne et al., 2008). During the pre-monsoon season, even though a marked diurnal wind breeze cycle was present at NCO-P, no significant average $O_3$ diurnal variation was observed. This probably indicated that during this season the contribution of air-masses transported from the lower troposphere by up-valley breezes almost equal the contribution of air-masses coming from the upper tropo-

sphere via down-valley breezes. During the summer monsoon, a significant $O_3$ maximum was observed at 10:00–11:00 with a minimum in the evening (at 20:00–21:00). This behaviour suggests the transport of air-masses richer in $O_3$ from along the valley or possibly influenced by a weak local photochemical production. In fact, $O_3$ concentrations decreased from 12:00, when cumulus formation usually developed at NCO-P (Bonasoni et al., 2010) reducing incoming solar radiation. $O_3$ reached a minimum concentration on 20:00–21:00, suggesting that destruction processes and/or surface deposition are dominant. The slightly higher $O_3$ levels observed during night-time were probably more representative for air-masses advected to NCO-P by the "large-scale" monsoon circulation (Bonasoni et al., 2010). In the post-monsoon season, the average $O_3$ diurnal cycle was characterised by a morning maximum (from 08:00 to 12:00) and a late afternoon minimum (18:00). Again, the low $O_3$ values during the afternoon were probably due to the transport of air-masses from the lower troposphere by up-valley winds ($V_y > 0$). On the other hand, comparing the average diurnal variations of $O_3$ and $V_y$, it is likely that the morning $O_3$ maximum could be the result of different contributions. In fact, $O_3$ concentrations peaked both under down-valley (at 08:00 LT) and up-valley (at 10:00–11:00 LT) breezes. While the first "bump" in the average $O_3$ peak was probably related to clean air-masses from the upper/free troposphere (as also suggested by the low BC average values of $50\ ng/m^3$, see Marinoni et al., 2010), the second $O_3$ "bump" was probably related to air-masses mixed by the developing up-valley breezes (as also suggested by the BC concentrations increasing from 50 to $200\ ng/m^3$, see Marinoni et al., 2010). In fact, as shown by Venzac et al. (2008), during the post-monsoon season ultrafine ($d_p$ of 10 nm or less) particle concentrations strongly increase after 11:00 LT, indicating new particle formation at the interface between ABL and "free tropospheric" air masses. The existence of systematic $O_3$ diurnal cycles at the NCO-P, mostly influenced by thermal circulation, was further supported by the analysis of the maxima/minima occurrence in function of day-time. In fact, for the four seasons (winter, pre-monsoon, monsoon and post-monsoon), 70–80% of the $O_3$ maxima were observed around the "peak" times indicated by the averaged $\Delta O_3$ reported in Fig. 4.

## 4 Climatological analysis of stratospheric intrusion at NCO-P

### 4.1 Identification of stratospheric intrusions at the NCO-P

For the purpose of identifying SI at NCO-P, different selection criteria were applied, according to the methodology presented by Cristofanelli et al. (2009). The detection algorithm was based on the analysis of in-situ $O_3$, AP and

RH, satellite-derived TCO daily values, and PV calculated along air-mass back-trajectories. In particular, days were selected that were characterised by the presence of air-masses with PV values exceeding the WMO definition of dynamical tropopause (i.e. PV>1.6 pvu, see WMO; 1986), and by significant variations of daily $O_3$, AP and TCO values over their seasonal cycles, as evaluated by applying a three-time repeated 19-day running mean (the so-called "Kolmogorov-Zurbenko" filter, see Sebald et al., 2000). In particular, we decided to select as influenced by possible SI, the days for which at least one of the 14 back-trajectories ending in a vertical range extending up to 50 hPa from the NCO-P altitude showed PV>1.6 pvu, basing on the experience gained in the analysis of case studies of stratospheric intrusions at other high mountain stations (Cristofanelli et al., 2006; Cui et al, 2009) and at the NCO-P itself (Bonasoni et al., 2009). With the aim of minimize the fraction of wrong selections, the considered tracers were analysed in groups of two (or more) and only simultaneous identification have been retained for the analysis. This approach appears to be reasonable since, as shown by previous investigations (Eisele et al., 1999; Zanis et al., 1999; Parrish et al., 2000), the downward transport of the stratospheric air-masses deep into the troposphere can be very complex, also including strong mixing between stratospheric and tropospheric air. In fact, only in a few very spectacular SI (see e.g. Bonasoni et al., 1999; Stohl et al., 2000) did all the tracers showed "clear" stratospheric signatures. Moreover, it should be noted that several studies (e.g. Schuepbach et al., 1999; Zachariasse at al., 2000; Ding and Wang, 2006; Zhu et al., 2006) stressed the importance of "sub-synoptic" processes (e.g. shear-induced differential advection, clear-air turbulence, mountain katabatic wind) in favouring the descent of air-masses from the stratosphere/upper-troposphere down to the middle troposphere. For these reasons and with the purpose of selecting the SI related to downward transport not associated with coherent airstreams, we also considered those days characterised by the co-presence of dry air-masses and elevated $O_3$ concentrations at the measurement site. To this aim we adopted an RH threshold of 60% to detect SI. Besides as being already applied at mountain stations to identify stratospheric air (e.g. Trickl et al., 2010), this value represents the typical "upper boundary" of RH at NCO-P able to contribute to the identification of SI events. Thus, different selection criteria were adopted in order to take into account expressly the possible mixing of stratospheric air-masses within the troposphere. In particular, a specific day was considered as being influenced by SI if enhanced daily $O_3$ mixing ratio was found and at least one of the following criteria was fulfilled:

– (i) significant variations of daily AP value AND the presence of back-trajectories with PV>1.6 pvu (26 days);

– (ii) presence of back-trajectories with PV>1.6 pvu AND significant TCO daily value increases (20 days);
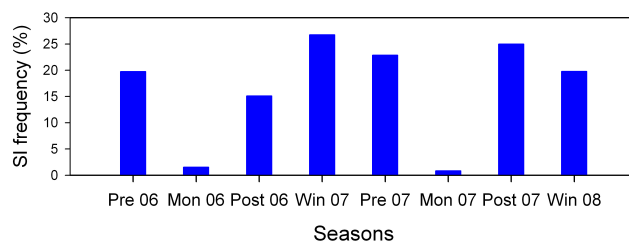


**Fig. 5.** Seasonal variation of SI frequency at NCO-P during the period March 2006–February 2008.

– (iii) significant variations of daily AP values AND significant TCO daily value increases (14 days);

– (iv) presence of RH<60% AND significant negative correlation $O_3$-RH AND daily $O_3$ maximum higher than the seasonal value AND significant variation of daily AP, PV or TCO values (84 days).

Considering that one specific day can be simultaneously selected by different criteria, 98 days (14.1% of the data-set) were retained as probably influenced by SI, a not negligible fraction of time. The simultaneous application of the four criteria identifies only air masses characterized by extremely clear stratospheric properties, while ignoring other weaker SI events, thus leading to the identification of a very low number of days (4) influenced by SI.

It should be noted that the last criterion was the most active in selecting possible SI. As being based on the analysis of not completely unambiguous stratospheric tracers (i.e. RH and $O_3$), we introduced additional thresholds (i.e. AP, PV, TCO) to minimize this ambiguity in the SI identifications. Moreover, we performed a sensitivity analysis by adopting different RH values. For instance, assuming the widely used 40% threshold for RH (e.g. Stohl et al., 2000; Trickl et al., 2010) the total number of selected SI reduced only by 2%. On the other side, the (iv) criterion should lead to the selection of further 15 SI days if the additional thresholds on AP, PV and TCO were not considered.

## 4.2 Seasonal frequency of stratospheric intrusions at NCO-P

Figure 5 shows the seasonal frequency of the number of days possibly affected by SI during the investigated period as deduced from the applied selection methodology. The highest seasonal SI frequency was recorded during non-monsoon seasons and in particular during the dry season 2007 (27% of the period). High frequency values were also recorded for the post-monsoon (25%) and pre-monsoon 2007 (23%). The lowest SI seasonal frequencies were detected during the monsoon seasons (less that 2%). As also suggested by the LAGRANTO atmospheric circulation analysis (Bonasoni et al., 2010), such behaviour probably reflects the role of the

SJS in promoting deep SI in the southern Himalayas. In fact, while during the summer monsoon the SJS was positioned on the northern side of the Tibetan Plateau (Schiemann et al., 2009), from October to May the axis of the SJS was situated between 25° N–30° N, thus being more likely to interact with the Himalayas. As deduced from this analysis, the seasonal SI frequencies during the 2-year investigation were rather constant at NCO-P (Fig. 5). Only for the post-monsoon seasons, was an evident variation of SI frequency observed from 2006 (SI frequency: 15%) to 2007 (SI frequency: 25%). By analysing the synoptic-scale air-mass circulation at NCO-P by means of the 3-D air-mass back-trajectory clusters presented by Bonasoni et al. (2010), it was found that during the post-monsoon 2007, the synoptic scale circulation was more influenced by fast-moving westerly air-masses originating over North Africa (W-NA cluster) than during the post-monsoon 2006 (31% versus 11% of occurrences). In agreement with Schiemann et al. (2009), who pointed out an elevated interannual variability for the SJS occurrence during autumn, this further indicated that strong westerly flows possibly related with the SJS can play an important role in determining SI in the southern Himalayas, even during the post-monsoon season. The leading role of SJS in favouring the transport of stratospheric air-masses to South Himalayas, is further described in a separate paper (Cristofanelli et al., in preparation) presenting the principal synoptic scenarios (i.e. upper tropospheric sub-tropical fronts, westerly moving disturbances, quasi-stationary ridges) promoting SI at the NCO-P during non-monsoon periods.

## 5 Influence of stratospheric intrusions on $O_3$ concentrations at NCO-P

During SI the stratospheric air-masses intruding into the troposphere are mixed with tropospheric air. In order to retain only the measurement periods actually influenced by stratospheric air-masses, for each day identified as influenced by SI, the 30-min RH and BC behaviours were analysed. In particular, to prevent photochemical $O_3$ in polluted air-masses transported to NCO-P by up-valley flows from influencing the estimate of "stratospheric" $O_3$, only those observations were considered that were characterised by RH<60% and BC<166 ng/m$^3$ (the 75th percentile of the yearly BC observations at NCO-P, see Marinoni et al., 2010). Based on this screening, during the 2-year periods (15 710 h) a total of 1591 h (10% of the analysed time period) were retained. If one assumes that during these periods the observed $O_3$ is entirely transported from the stratosphere, a rough estimate can be inferred as to the contribution of SI in determining the tropospheric $O_3$ levels in the southern Himalayas. On Table 2, for all the investigated period and for each season, the average $O_3$ concentrations associated with SI are showed. The seasonal $O_3$ concentrations associated with SI showed the highest values during the pre-monsoon 2006 (70±8 ppbv,
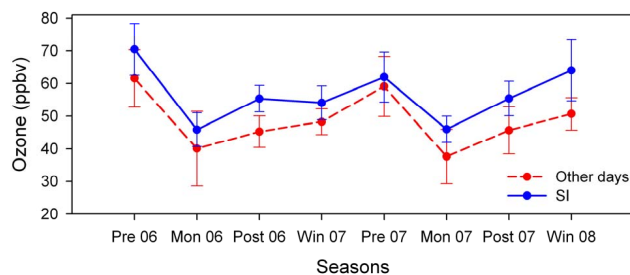


**Fig. 6.** Average $O_3$ concentrations recorded during SI and during periods not affected by SI (Other days) at NCO-P for the period March 2006–February 2008. Vertical bars represent the standard deviations.

N: 550) and dry season 2007 (64±9 ppbv, N: 562), with a cycle which resembles the typical yearly $O_3$ variations observed at the measurement site (Fig. 6). On average, a mean $O_3$ concentration of 61±9 ppbv ($N = 3183$) was observed, corresponding to a significant excess of +27.1% (+13 ppbv), compared to periods not affected by SI. The seasonal net $O_3$ increase (expressed as percentage) recorded during SI with respect to periods not affected by such phenomena (Table 2) shows a seasonal cycle with the highest values during the post-monsoon (+22.0%, equivalent to +10 ppbv) and the lowest during the pre-monsoon (+8.6%, equivalent to + 5 ppbv). It is worth noting that the small average $O_3$ increases were observed during the pre-monsoon seasons, which could seem in contrast with the high average $O_3$ concentrations recorded during this season for SI (Table 2). However, one should bear in mind that, particularly during the pre-monsoon season, high photochemical $O_3$ concentrations due to anthropogenic pollution and biomass burning strongly affect South Asia and the southern Himalayas, as also observed at NCO-P (see Bonasoni et al., 2010). Assuming that during SI all the observed $O_3$ can be traced back to the stratosphere, for the purpose of calculating the upper limit of the fraction of tropospheric $O_3$ due to SI at NCO-P, following Elbern et al. (1997), the maximum integral stratospheric contribution $O_{3S}$ was defined as:

$$O_{3S} = \sum_{i=1}^{n} \sum_{t=-T_i/2}^{T_i/2} O_3(t) \qquad (1)$$

where for each season, $O_3(t)$ denoted the 30-min $O_3$ concentrations recorded during the $i^{th}$ event with time length $T_i$ (expressed as number of 30-min values). The results, expressed as ppbv*h, are reported in Table 2. The $O_{3S}$ seasonal cycle was characterised by maximum values during the pre-monsoon and dry seasons, minimum values during the monsoon and post-monsoon, and a strong peak-to-peak amplitude (seasonal maximum to minimum ratio ≈26). This was in good agreement with the model experiment of Lelieveld et al. (2009), who showed a minimum of stratospheric originated $O_3$ during the summer period (July–September) over

the Himalayas. The relative contribution of SI to the $O_3$ burden over the southern Himalayas can be estimated by calculating the seasonal enhancement ratio between $O_{3S}$ and the integral $O_3$ amount recorded outside SI (hereinafter $O_{3NS}$). The resulting values are reported in Table 2, where the seasonal enrichment ratios $O_{3S}/O_{3NS}$ are expressed as percentages. Over the 2-year period, the average value of the enrichment ratio $O_{3S}/O_{3NS}$ was 13.7%. The contribution of SI to the tropospheric $O_3$ as evaluated by the $O_{3S}/O_{3NS}$ ratio shows a pronounced seasonal cycle, with a minimum during the monsoon (<0.1%), a maximum during the winter (up to 24.2%) and intermediate but not-negligible values during the pre-monsoon (up to 19.2%) and post-monsoon (up to 12.6%).

## 6 Discussion and conclusions

The work presents the first 2 years (March 2006–February 2008) of continuous $O_3$ observations at the Nepal Climate Observatory - Pyramid (NCO-P, 5079 m a.s.l., Nepal). With the aim of contributing to clarifying the role played by transport processes in determining the $O_3$ levels and variability in one of the world's most critical high-altitude regions, a systematic assessment was performed of the influence of SI on $O_3$ concentrations recorded at this GAW-WMO station, which is considered representative of the Southern Himalayas remote troposphere. As $O_3$ is a powerful greenhouse gases and a dangerous pollutant and due to the increasing emissions of anthropogenic $O_3$ precursors over South Asia (Ohara et al., 2007), such activity appears to be particularly important also considering that this region is strongly influenced by one of the so-called Atmospheric Brown Clouds, with severe implications on regional climate, air-quality and food security (Ramanathan et al., 2008).

As deduced from the analysis of 30-min average values (49±12 ppbv, N = 31420), the seasonal $O_3$ behaviour was found to be characterised by a maximum during the pre-monsoon (61±9 ppbv, N = 9376) and a minimum during the monsoon (39±10 ppbv, N = 10836) seasons. As shown by Bonasoni et al. (2010), such seasonal variation is partially influenced by the synoptic-scale atmospheric circulation related to the South Asia monsoon regime. In fact, during summer air-masses poor in $O_3$ were transported from lower latitudes to the southern Himalayas, while during the pre-monsoon the measurement site was mostly affected by westerly air-masses originating from North Africa, Middle East, Central Asia and Northern India as well. In addition to long-range transport, the efficient day-time valley wind circulation (see Bonasoni et al., 2010; Marinoni et al., 2010) can play an important role in transporting polluted air-masses rich in $O_3$ to NCO-P. Thus, the correct identification of the measurement periods influenced by such pollution transport is fundamental for quantifying the exact contribution of long-range transport processes (like SI) on the observed $O_3$ levels.

To identify the days possibly influenced by SI, analyses were performed of *in-situ* observations of $O_3$, RH, AP, satellite-derived OMI-TCO data and PV values provided by the LAGRANTO back-trajectory model. After defining an appropriate threshold value for each tracer, different selection criteria were applied to identifying possible SI days at NCO-P. In summary, during the 2-year investigation, 14.1% of the analysed days turned out to be affected by SI. These results appeared slightly higher than showed in Cristofanelli et al. (2009) who used a similar approach for analysing one-year of data at the same measurement site, thus suggesting that our estimate of the SI frequency directly affecting South Himalayas is quite robust. Considering the high altitude of the measurement site (5079 m a.s.l.), the values may appear low, if compared with the SI frequencies (ranging from 5% to 40%) inferred at high mountain stations located in Europe (with altitudes ranging from 2100 to 3800 m a.s.l., see Stohl et al., 2000; Cristofanelli et al., 2006; Cui et al., 2009; Trickl et al., 2010). It could indicate that the southern Himalayas is not among the world regions most affected by SI. On applying a less restrictive methodology, which excluded the threshold on $O_3$ concentrations (following Cristofanelli et al., 2006 and Trickl et al., 2010), the occurrence of days affected by SI increased to 30%. Nevertheless, our SI frequency estimate appears to be in good qualitative agreement with the modelling analyses performed by Sprenger and Wernli (2003), which showed that the probability of a deep SI affecting the NCO-P region is three time less than over western and central Europe, an area characterized by frequent cyclogenesis episodes and often directly impacted by the intense polar jet stream (e.g. Schuepbach et al., 1999; Sprenger and Wernli, 2003). Moreover, the Europe is located at the end of the North Atlantic storm track region, where PV streamer usually occur (Wernli and Sprenger, 2007). As deduced from the present analysis, a strong seasonal cycle characterizes the frequency of SI days with a minimum during the monsoon season (1.2%) and higher values during the rest of the year (21.5%). Bonasoni et al. (2010) showed that during non-monsoon seasons, the NCO-P area is significantly affected by westerly air-masses. Therefore, the results obtained here reflect the role of the SJS in promoting deep SI over the southern Himalayas. In fact, during the summer monsoon the SJS is positioned on the northern side of the Tibetan Plateau, while from October to May the axis of the SJS is usually between 25° N–30° N (Schiemann et al., 2009; Ding and Wang, 2006). In particular, the presence of the upper tropospheric sub-tropical front, westerly moving disturbances and, quasi-stationary ridges represent the principal synoptic scenarios able to induce SI at the NCO-P during non-monsoon periods. On the other hand, the few SI events during the monsoon period are likely to be related to the occurrence of a monsoon depression over the Bay of Bengal and Northern Indian plains. Finally, with the aim of evaluating the occurrence of SI also in terms of events, time periods consisting of contiguous SI days were defined

**Table 2.** For periods affected by SI at the NCO-P: seasonal averaged $O_3$ concentration ($O_3$), number of 30-min observations (N), $O_3$ excess ($\Delta O_3$) and maximum $O_3$ integral ($O_{3S}$, see Sect. 5 for definition). Seasonal averaged integral $O_3$ outside SI ($O_{3NS}$) and seasonal maximum $O_3$ enhancement ratios ($O_{3S}/O_{3NS}$) at NCO-P are also reported.

| Periods | $O_3$ (ppbv) | N | $\Delta O_3$ (%) | $O_{3S}$ (ppbv*h) | $O_{3NS}$ (ppbv*h) | $O_{3S}/O_{3NS}$ (%) |
|---------|--------------|-----|----------|-------------------|--------------------|----------------------|
| All seasons | $61\pm9$ | 3183 | +27.1 | $9.7\times10^4$ | $7.0\times10^5$ | 13.7% |
| Pre-monsoon | $65\pm9$ | 1396 | +8.6 | $4.5\times10^4$ | $2.4\times10^5$ | 19.2% |
| Monsoon | $46\pm9$ | 73 | +18.0 | $1.7\times10^3$ | $2.2\times10^5$ | <0.1% |
| Post-monsoon | $55\pm9$ | 373 | +22.0 | $1.0\times10^4$ | $8.1\times10^4$ | 12.6% |
| Winter season | $58\pm9$ | 1341 | +17.2 | $3.9\times10^4$ | $1.6\times10^5$ | 24.2% |

as "SI events": a total of 42 SI events were observed (19 during 2006 and 23 during 2007). The average time-length of the identified events was 2.3 days, with 80% of detected events having a time duration of less than 2 days.

With the aim of estimating the contribution of SI on $O_3$ levels at the NCO-P for the 2-year investigation period, the 30-min $O_3$, BC and RH data-sets were analysed. It should be noted that in this analysis we assessed the contribution from relatively "fresh" SI, for which still clear stratospheric "fingerprints" were observable. In particular, to prevent measurement periods possibly affected by anthropogenic transported pollution from influencing the estimate, data with high RH and BC, indicating the transport of polluted and wet air-masses by up-valley breezes, were not considered. On average, the days influenced by possible air-mass transport from the stratosphere showed a significant net $O_3$ increase of 27.1% (+13 ppbv) with respect to periods not affected by SI. In addition, the results indicated that the average net $O_3$ increases related to SI were characterized by a clear annual variation, with the highest values during the post-monsoon (+22.0%) and the lowest during the pre-monsoon (+8.6%). In order to calculate the maximum fraction of tropospheric $O_3$ due to SI at NCO-P, the integral stratospheric $O_3$ contribution ($O_{3S}$) was calculated basing on the assumption that all the $O_3$ observed at the NCO-P during an SI can be traced back to the stratosphere. Through this analysis it was estimated that up to 13.7% of surface $O_3$ recorded at NCO-P can be attributed to SI. On a seasonal basis, the lowest SI contributions were found during the summer monsoon (less than 0.1%), while the highest were found during winter (up to 24.2%). Such values, which represent an upper limit of the $O_3$ contributions by SI at NCO-P, are in good agreement with the results of Sudo and Akimoto (2007) who, by running a tagged tracer simulation with a global chemical transport model, estimated that STE contributed from 10% to 20% of the annual TCO over the southern Himalayas. However, it should be noted that the present estimates can vary if a different SI selection methodology is applied to screen SI at NCO-P or if different measures of the stratospheric $O_3$ input are considered. In particular, with the purpose of defining the lowest limit of SI contribution to surface $O_3$ at NCO-P,

we adopted the very conservative assumption that during an SI only the observed $O_3$ excess ($\Delta O_3$) can be traced back to the stratosphere. In this case, on a yearly basis, the 2% of surface $O_3$ could be directly attributed to SI.

In the framework of the ABC project, the presented results contribute to filling the gap in knowledge concerning this important pollutant/regional greenhouse gas over the high Himalayas, providing the basis for a better evaluation of its contribution to the radiative forcing and air-quality in this critical region (Ramanthan et al., 2008). Even if the present estimates are associated to a rather large uncertainties, the obtained results suggest that SI can play a not-negligible role in determining the levels and variability of tropospheric $O_3$ over the southern Himalayas, therefore having significant potential impacts on the regional radiative budget, particularly during the strongest events. Thus, in evaluating future scenarios of climate variations, the influence of SI contributions to tropospheric $O_3$ cannot be omitted. However, other processes (e.g. long-distance and regional transport of air pollution, see Bonasoni et al., 2010, and Marinoni et al., 2010) could play an important role in determining $O_3$ levels over the southern Himalayas. Further work will be deserved to investigate the overall contribution of polluted air-masses to the $O_3$ concentrations observed at NCO-P, thus providing up-to-date information on the role played by anthropic emissions in influencing $O_3$ variations in this important geographical area.

Edited by: J. J. Schauer

# References

Agrawal, M., Auffhammer, M., Chopra, U. K., Emberson, L., Iyngararasan, M., Kalra, N., Ramana, M. V., Ramanathan, V., Singh, A. K., and Vincent, J.: Impacts of Atmospheric Brown Clouds on Agriculture, Part II of Atmospheric Brown Clouds: Regional Assessment Report with Focus on Asia, Project Atmospheric Brown Cloud, UNEP, Nairobi, Kenya, 2008.

Bonasoni, P., Evangelisti, F., Bonafé, U,. Ravegnani, F., Calzolari, F., Stohl, A., Tositti, L., Tubertini, O., and Colombo, T.: Stratospheric ozone intrusion episodes recorded at Mt. Cimone during VOTALP project: case studies. Atmos. Environ., 34, 1355–1365, 1999.

Bonasoni, P., Laj, P., Angelini, F., Arduini, J., Bonafè, U., Calzolari, F., Cristofanelli, P., Decesari, S., Facchini, M.C., Fuzzi, S., Gobbi, G. P., Maione, M., Marinoni, A., Petzold, A., Roccato, F., Roger, J. C., Sellegri, K., Sprenger, M., Venzac, H., Verza, G. P., Villani, P., and Vuillermoz, E.: The ABC-Pyramid Atmospheric Research Observatory in Himalaya for aerosol, ozone and halocarbon measurements, Sci. Total Environ., 391, 241–251, 2008.

Bonasoni, P., Laj, P., Marinoni, A., Sprenger, M., Angelini, F., Arduini, J., Bonafè, U., Calzolari, F., Colombo, T., Decesari, S., Di Biagio, C., di Sarra, A. G., Evangelisti, F., Duchi, R., Facchini, M. C., Fuzzi, S., Gobbi, G. P., Maione, M., Panday, A., Roccato, F., Sellegri, K., Venzac, H., Verza, G. P., Villani, P., Vuillermoz, E., and Cristofanelli, P.: Atmospheric Brown Clouds in the Himalayas: first two years of continuous observations at the Nepal-Climate Observatory at Pyramid (5079 m), Atmos. Chem. Phys. Discuss., 10, 4823–4885, doi:10.5194/acpd-10-4823-2010, 2010.

Böhner, J.: General climatic controls and topoclimatic variations in Central and High Asia. BOREAS, 35, 279–294, 2006.

Conti, S., Meli, P., Minelli, G., Solimini, R., Toccaceli, V., Vichi, M., Beltrano, C., and Perini, L.: Epidemiologic study of mortality during the Summer 2003 heat wave in Italy, Environ. Res., 98, 390–399, 2005.

Cristofanelli, P., Bonasoni, P., Tositti, L., Bonafè, U., Calzolari, F., Evangelisti, F., Sandrini, S., and Stohl, A.: A 6-year analysis of stratospheric intrusions and their influence on ozone at Mt. Cimone (2165 m above sea level), J. Geophys. Res., 111, D03306, doi:10.1029/2005JD006553, 2006.

Cristofanelli, P., Bonasoni, P., Bonaf≝'e, U., Calzolari, F., Duchi, R., Marinoni, A., Roccato, F., Vuillermoz, E., and Sprenger, M.: Influence of lower stratosphere/upper troposphere (LS/UT) transport events on surface ozone at the Everest-Pyramid GAW Station (Nepal, 5079 m a.s.l.): first year of analysis, Int. J. Rem. Sens., 30(15), 4083–4097, 2009.

Cristofanelli, P., Bracci, A., Sprenger, M., Bonafè, U., Calzolari, F., Duchi, R., Marinoni, A., Roccato, F., Vuillermoz, E., and Bonasoni, P.: Case studies of stratospheric intrusions at the Nepal Climate Observatory - Pyramid (Himalaya, 5079 m a.s.l.): a synoptic-scale investigation, in preparation, 2010.

Cui, J., Sprenger, M., Staehelin, J., Siegrist, A., Kunz, M., Henne, S., and Steinbacher, M.: Impact of stratospheric intrusions and intercontinental transport on ozone at Jungfraujoch in 2005: comparison and validation of two Lagrangian approaches, Atmos. Chem. Phys., 9, 3371–3383, doi:10.5194/acp-9-3371-2009, 2009.

Danielsen, E. F.: Stratospheric-Tropospheric exchange based on radioactivity, ozone and potential vorticity, J. Atmos. Sci., 25, 502–518, 1968.

Davies, T. D. and Schuepbach, E.: Episodes of high ozone concentrations at the Earth's surface resulting from transport down from the upper troposphere/lower stratosphere, Atmos. Environ., 28, 53–68, 1994.

Ding, D. and Wang, T.: Influence of stratosphere-to-troposphere exchange on the seasonal cycle of surface ozone at Mount Waliguan in western China, Geophys. Res. Lett., 33, L03803, doi:10.1029/2005GL024760, 2006.

Eisele, H., Scheel, H. E., Sladkovic, R., and Trickl, T.: High resolution Lidar measurements of stratosphere-troposphere exchange, J. Atmos. Science, 56, 319–330, 1999.

Elbern, H., Kowol, J., Sladkovic, R., and Ebel, A.: Deep stratospheric intrusions: a statistical assessment with model guided analysis, Atmos. Environ., 31, 3207–3226, 1997.

Fischer, H., Kormann, R., Klüpfel, T., Gurk, C., Königstedt, R., Parchatka, U., Mühle, J., Rhee, T. S., Brenninkmeijer, C. A. M., Bonasoni, P., and Stohl, A.: Ozone production and trace gas correlations during the June 2000 MINATROC intensive measurement campaign at Mt. Cimone, Atmos. Chem. Phys., 3, 725–738, doi:10.5194/acp-3-725-2003, 2003.

Forster, P., Ramaswamy, V., Artaxo, P., Berntsen, T., Betts, R., Fahey, D. W., Haywood, J., Lean, J., Lowe, D. C., Myhre, G., Nganga, J., Prinn, R., Raga, G., Schulz M., and Van Dorland, R.: Changes in Atmospheric Constituents and in Radiative Forcing, in Climate Change 2007: The Physical Science Basis. Contribution of Working Group I to the Fourth Assessment Report of the Intergovernmental Panel on Climate Change, edited by: Solomon, S., Qin, D., Manning, M., Chen, Z., Marquis, M., Averyt, K. B., Tignor M., and Miller, H. L., Cambridge University Press, Cambridge, UK and New York, NY, USA, 129–234, 2007.

Fuhrer, J. and Booker, F.: Ecological issues related to ozone: agricultural issues, Environ. Int., 29, 141–154, 2003.

Gauss, M., Myhre, G., Pitari, G., et al:. Radiative forcing in the 21$^{st}$ century due to ozone changes in the troposphere and the lower stratosphere, J. Geophys. Res., 108, 4292, doi:10.1029/2002JD002624, 2003.

GAW: report of the WMO meeting of experts on the quality assurance plan for the Global Atmospheric Watch (GAW), Garmisch-Partenkirchen, Germany, 26–30 March, 1992.

Han, Z., Chongping, H., Libo, Z., Wei, W., and Yongxiao, J.: ENSO signal in total ozone over Tibet. Adv. Atmos. Sci., 18, 231–238, 2001.

Henne, S., Klausen, J., Junkermann, W., Kariuki, J. M., Aseyo, J. O., and Buchmann, B.: Representativeness and climatology of carbon monoxide and ozone at the global GAW station Mt. Kenya in equatorial Africa, Atmos. Chem. Phys., 8, 3119–3139, doi:10.5194/acp-8-3119-2008, 2008.

Hoek, G., Fisher, P., Brunekreef, B., Lebret, E., Hofsschreuder, P., and Mennen, M. G.: Acute effects of ambient ozone on pulmonary function of children in The Netherlands, Am. Rev. Respire. Discuss., 147, 11–117, 1993.

Jacobson, M. Z.: Atmospheric Pollution: history, science and regulation. Cambridge University Press, Cambridge, United Kingdom and New York, NY, USA, 2002.

Klausen, J., Zellweger, C., Buchmann, B., Hofer, P.: Uncertainty and bias of surface ozone measurements at selected Global Atmosphere Watch sites, J. Geophys. Res., 108 (D19), 4622, doi:10.1029/2003JD003710, 2003.

Lelieveld, J., Hoor, P., Jöckel, P., Pozzer, A., Hadjinicolaou, P., Cammas, J.-P., and Beirle, S.: Severe ozone air pollution in the Persian Gulf region, Atmos. Chem. Phys., 9, 1393–1406, doi:10.5194/acp-9-1393-2009, 2009

Levelt, P. F., van Den Oord, g. H. J., Dobber, M. R. , Malkki, A., Visser, H., de Vries, J., Stammes, P., Lundell, j. O. V., and Saari, H.: The Ozone Monitoring Instrument. IEEE Trans. Geosci. Remote Sens., 44, 1093–1101, doi:10.1109/TGRS.2006.872333, 2006.

Levelt, P. F., Hilsenrath, E., Leppelmeier, G. W., van Den Oord, G. H. J., Bhartia, P. K., Tamminen, J., de Haan, J. F., and Veefkind, J. P.: Science objectives of the Ozone Monitoring Instrument, IEEE Trans. Geosci. Remote Sens., 44, 1199–1208, doi:10.1109/TGRS.2006.872336, 2006.

Loring, R. O. J., Fuelberg, H. E., Fishman, J., Watson, M. V., and Browell, E. V.; Influence of a middle-latitude cyclone on tropospheric ozone distributions during a period of TRACE A, J. Geophys. Res., 101(D19), 23941–23956, 1996.

Marinoni, A., Cristofanelli, P., Laj, P., Duchi, R., Calzolari, F., Decesari, S., Sellegri, K., Vuillermoz, E., Verza, G. P., Villani, P., and Bonasoni, P.: Aerosol mass and black carbon concentrations, two year-round observations at NCO-P (5079 m, Southern Himalayas), Atmos. Chem. Phys. Discuss., 10, 8379–8413, doi:10.5194/acpd-10-8379-2010, 2010.

Mickley, L. J., Jacob, D. J., Field, B. D., and Rind, D.: Climate response to the increase in tropospheric ozone since preindustrial times: A comparison between ozone and equivalent CO2 forcings, J. Geophys. Res., 109, D05106, doi:1029/2003JD003653, 2004.

Miyazaki, K., Iwasaki, T., Shibata, K., and Deushi, M.: Roles of transport in the seasonal variation of the total ozone amount, J. Geophys. Res., 110, D18309, doi:10.1029/2005JD005900, 2005.

Moore, G. W. K. and Semple, J. L.: High Himalayan meteorology: Weather at the South Col of Mount Everst, Geophis. Res. Lett., 31, L18109, doi:10.1029/2004GL020621, 2004.

Moore, G. W. K. and Semple, J. K.: A Tibetan Taylor Cap and a halo of stratospheric ozone over Himalya, Geophys. Res. Lett., 32, L21810, doi:10.1029/2005GL024186, 2005.

Ohara, T., Akimoto, H., Kurokawa, J., Horii, N., Yamaji, K., Yan, X., and Hayasaka, T.: An Asian emission inventory of anthropogenic emission sources for the period 1980–2020, Atmos. Chem. Phys. 7, 4419–4444, doi:10.5194/acp-7-4419-2007, 2007.

Olsen, M. A., Gallus, W. A., Stanford, J. L., and Brown, J. M.: Fine-scale comparison of TOMS total ozone data with model analysis of an intense Midwestern cyclone. J. Geophys. Res., 105, 20487–20498, 2000.

Paoletti, E.: Impact of ozone on Mediterranean forests: A review, Environ. Poll., 144, 463–474, 2006.

Parrish, D., Holloway, J., Jakoubek, R., Trainer, M., Ryerson, T., Hübler, G., Fehsenfeld, F., Moody, J., and Cooper, O.: Mixing of anthropogenic pollution with stratospheric ozone: A case study from the North Atlantic wintertime troposphere, J. Geophys. Res., 105(D19), 24363-24374, 2000.

Petzold, A., Kramer, H., and Schönlinner, M.: Continuous measurement of atmospheric black carbon using a multi-angle absorption photometer, Environ. Sci. Pollut. Res., 4, 78–82, 2002.

Ramanathan, V., Agrawal, M., Akimoto, H., et al.: Atmospheric Brown Clouds: Regional Assessment Report with Focus on Asia. Published by the United Nations Environment Programme, Nairobi, Kenya, 2008.

Roelofs, G.-J., and Lelieveld, J.: Model study of the influence of cross-tropopause O$_3$ transports on tropospheric O$_3$ levels, Tellus, 49B, 38–55, 1997.

Schiemann, R., Lüthi, D., and Schär, C.: Seasonality and Interannual Variability of the Westerly Jet in the Tibetan Plateau Region, J. Climate, 22, 2940–2957, 2009.

Schoeberl, M. R., Douglass, A. R., Hilsenrath, E., et al.: Overview of the EOS-Aura mission. IEEE Trans.. Geosci. Remote Sens., 44, 1066–1074, doi:10.1109/TGRS.2005.861950, 2006.

Schuepbach, E., Davies, T. D., and Massacand, A. C.: An unusual springtime ozone episode at high elevation in the Swiss Alps: contributions both from cross-tropopause exchange and from the boundary layer, Atmos. Environ., 33, 1735–1744, 1999.

Sebald, L., Treffeisen, R., Reimer, E., and Hies, T.: Spectral analysis of air pollutants, Part 2: ozone time series. Atmos. Environ., 34, 3503–3509, 2000.

Sprenger, M., Croci Maspoli, M., and Wernli, H.: Tropopause folds and cross-tropopause exchange: A global investigation based upon ECMWF analyses for the time period March 2000 to February 2001, J. Geophys. Res., 108(D12), 8518, doi:10.1029/2002JD002587, 2003.

Sprenger, M. and Wernli, H.: A northern hemispheric climatology of cross-tropopause exchange for the ERA15 time period (1979–1993), J. Geophys. Res., 108(D12), 8521, doi:10.1029/2002JD002636, 2003.

Sprenger, M., Wernli, H., and Bourqui, M.: Stratosphere-troposphere exchange and its relation to potential vorticity streamers and cutoffs near the extratropical tropopause, J. Atmos. Sci., 64, 1587–1602, 2007.

Stohl, A., Spichtinger-Rakowsky, N., Bonasoni, P., Feldmann, H., Memmesheimer, M., Scheel, H. E., Trickl, T., Hubener, S., Ringer, W., and Mandl, M.: The influence of stratospheric intrusions on alpine ozone concentrations. Atmos. Environ., 34, 1323–1354, 2000.

Sudo, K. and Akimoto, H.: Global source attribution of tropospheric ozone: Long-range transport from various source regions, J. Geophys. Res., 112, D12302, doi:10.1029/2006JD007992, 2007.

Tanimoto, H., Sawa, Y., Matsueda, H., Uno, I., Ohara, T., Yamaji, K., Kurokawa, J., and Yonemura, S.: Significant latitudinal gradient in the surface ozone spring maximum over East Asia, Geophys. Res. Lett., 32, L21805, doi:10.1029/2005GL023514, 2005.

Tian, W., Chipperfield, M., and Huang, Q.: Effects of the Tibetean Plateau on total column ozone distribution. Tellus, 60B, 622–235, 2008.

Trickl, T., Feldmann, H., Kanter, H.-J., Scheel, H.-E., Sprenger, M., Stohl, A., and Wernli, H.: Forecasted deep stratospheric intrusions over Central Europe: case studies and climatologies, Atmos. Chem. Phys., 10, 499–524, doi:10.5194/acp-10-499-2010, 2010.

Venzac, H. Sellegri, K., Laj, P., Villani, P., Bonasoni, P., Marinoni, A., Cristofanelli, P., Calzolari, F., Fuzzi, S., Decesari, S., Facchini, M.-C., Vuillermoz, E., and Verza, G. P.: High Frequency new particle formation in the Himalayas, PNAS, 105 (41), 15666–15671, 2008.

Wahid, A., Milne, E., Shamsi, S. R. A., Ashmore, M. R., and Marshall, F. M.: Effext of oxidants on soybean growth and yield in Pakistan, Environ. Poll., 113, 271–280, 2001.

Wang, T., Wong, H. L. A., Tang, J., Ding, A., Wu, W. S., and Zhang, X. C.: On the origin of surface ozone and reactive nitrogen observed at a remote mountain site in the northeastern Qinghai-Tibetan Plateau, western China, J. Geophys. Res., 111(D8), D08303, doi:10.1029/2005JD006527, 2006.

Wernli, H. and Davies, H: A Lagrangian-based analysis of extratropical cyclones. Part I: The method and some applications, Q. J. Roy. Meteor. Soc., 123, 467–489, 1997.

Wernli, H. and Sprenger, M.: Identification and ERA-15 climatology of potential vorticity streamers and cutoffs near the extratropical tropopause, J. Atmos. Sci., 64, 1569–1586, 2007.

West, J. J., Naik, V., Horowitz, L. W., and Fiore, A. M.: Effect of regional precursor emission controls on long-range ozone transport – Part 2: Steady-state changes in ozone air-quality and impacts on human mortality. Atmos. Chem. Phys., 9, 6095–6107, doi:10.5194/acp-9-6095-2009, 2009.

Wild, O.: Modelling the global tropospheric ozone budget: exploring the variability in current models. Atmos. Chem. Phys., 7, 2643–2660, doi:10.5194/acp-7-2643-2007, 2007.

Wimmers, A. J. and Moody, J. L.: Tropopause folding at satellite-observed spatial gradients: 1. Verification of an empirical relationship, J. Geophys. Res., 109, D19306, doi:10.1029/2-3JD004145, 2004.

Wotawa, G., Kroger, H., and Stohl, A.: Transport towards the Alps - results from trajectory analyses and photochemical model studies, Atmos. Environ., 34, 1367–1377, 2000.

World Meteorological Organization (WMO): Atmospheric ozone 1985: Global ozone research and monitoring report, WMO Rep. 16, Geneva, Switzerland, 1986.

Zanis, P., Schuenpbach, E., Gaeggeler, H. W., Huebener, S., and Tobler, L.: Factors controlling Beryllium-7 at Jungfraujoch in Switzerland, Tellus, 51(4), 789–805, 1999.

Zachariasse, M., van Velthoven, P. F. J., Smit, H. G. J, Lelieveld, J., Mandal, T. K., and Kelder H.: Influence of stratosphere-troposphere exchange on tropospheric ozone over the tropical Indian Ocean during the winter monsoon, J. Geophys. Res., 105(D12), 15403–15416, 2000.

Zhu, T., Lin, W., Song, Y., Cai, X., Zou, H., Kang, L., Zhou, L., and Akimoto, H.: Downward transport of ozone-rich air near Mt. Everest, Geophys. Res. Lett., 33, L23809, doi:10.1029/2006GL027726, 2006.